

1 **Fluvio-deltaic avulsions during relative sea-level fall**

2 A.G. Nijhuis¹, D.A. Edmonds², R.L. Caldwell², J.A. Cederberg³, R.L. Slingerland³, J.L. Best⁴,
3 D.R. Parsons⁵, and R.A.J. Robinson⁶

4
5 ¹*Department of Earth and Environmental Sciences, 140 Commonwealth Ave, Boston College,*
6 *213 Devlin Hall, Chestnut Hill, MA 02467*

7
8 ²*Indiana University Department of Geological Sciences and Center for Geospatial Data*
9 *Analysis, 1001 East 10th St. Office GY425, Bloomington, IN, 47405, USA.*

10
11 ³*Department of Geosciences, The Pennsylvania State University, University Park, Pennsylvania*
12 *16802, USA.*

13
14 ⁴*Departments of Geology, Geography and Geographic Information Science, Mechanical Science*
15 *and Engineering and Ven Te Chow Hydrosystems Laboratory, University of Illinois, 133*
16 *Computer Applications Bldg, 605 E. Springfield Ave., Champaign, IL 61820*

17
18 ⁵*Department of Geography, Environment and Earth Sciences, University of Hull, Cottingham*
19 *Road, Hull, HU6 7RX*

20
21 ⁶*Department of Earth & Environmental Sciences, University of St Andrews, Irvine Building,*
22 *North Street, St Andrews, Fife KY16 9AL, Scotland, UK*

23
24 **ABSTRACT**

25 Understanding river response to relative sea-level (RSL) changes is essential for predicting
26 fluvial stratigraphy and source to sink dynamics. Recent theoretical work has suggested that
27 during RSL fall rivers can remain aggradational. However, field data are needed to verify this
28 response and investigate sediment deposition processes. We show with field work and modeling
29 that during RSL fall fluvio-deltaic systems can remain aggradational or at grade, leading to
30 superelevation and delta lobe avulsions. Our field site is the Goose River in Newfoundland-
31 Labrador, which has experienced steady RSL fall of around 3 to 4 mm yr⁻¹ in the past 5 ka from
32 post-glacial isostatic rebound. Elevation analysis and optically-stimulated luminescence dating
33 suggest that during RSL fall the Goose River avulsed and deposited three delta lobes. Model

34 results from Delft3D show that if the characteristic system fluvial response time is longer than
35 the duration of RSL fall, then rivers remain aggradational or at grade and continue to avulse due
36 to superelevation. Intriguingly, our results also suggest that avulsions become more frequent at
37 faster RSL fall rates, provided the system response time remains longer than RSL fall duration.
38 This work suggests that the rate of RSL fall may play an important role in setting the architecture
39 of falling stage deposits.

40

41 **INTRODUCTION**

42 Predicting how rivers erode or deposit sediment in response to relative sea-level (RSL)
43 change is critical for understanding sequence stratigraphy (Catuneanu, 2006) and source to sink
44 dynamics (Romans and Graham, 2013). Despite this importance, it is unclear if during RSL fall
45 rivers incise and bypass sediment to the deep marine (e.g. Vail, 1977), or if they deposit
46 sediment on the coastal plain starving the deep marine (e.g. Holbrook and Bhattacharya, 2012).
47 In the latter case, strata deposited during RSL fall are typically terraced deposits with a
48 descending shoreline trajectory (Posamentier and Morris, 2000; Catuneanu, 2006; Helland-
49 Hansen and Hampson, 2009, Li and Bhattacharya, 2013). While the incisional model has
50 received considerable attention, there is mounting theoretical evidence (Muto and Steel, 2004)
51 that deposition during RSL fall may be common, yet few studies have focused on the processes
52 that deposit these sediments.

53 For example, experimental work shows that a coastal river with constant sediment
54 supply, prograding over a linear basin slope, does not just incise during steady RSL fall. Instead
55 the river experiences an autogenic response of multiple episodes of deltaic lobe deposition,
56 incision through the lobe, and abandonment (van Heijst and Postma, 2001; Muto and Steel, 2002,

57 2004; Swenson and Muto, 2007). But, these ideas have not been tested on field-scale rivers, nor
58 have they been investigated with channel-resolving morphodynamic models.

59 Our goal here is to understand the processes that control sediment deposition during RSL
60 fall by combining elevation analysis, and optically stimulated luminescence (OSL) data from the
61 modern Goose River, Newfoundland-Labrador, and morphodynamic modeling. Our
62 observations show that as RSL falls Goose River avulsions create multiple delta lobes at
63 progressively lower elevations. Delft3D models simulating RSL fall confirm these field
64 observations and suggest that the number and size of delta lobes scale with the rate of RSL fall.

65

66 **STUDY AREA**

67 The Goose River empties into Goose Bay at the western edge of Lake Melville—a fjord-
68 type estuary located 200 km inland of the Labrador Sea, Labrador, Canada (Liverman, 1997)
69 (Fig. 1). The majority of Goose Bay water depths range between 20 m and 40 m, but nearshore
70 depths shallow to 10 m (Blake, 1956). The bay is stratified with a 5 m-thick stable fresh water
71 surface layer overlaying saline bottom waters. The tidal amplitude within Goose Bay is ~0.4 m
72 (Vilks et al., 1987). The Goose River has a drainage area of 3,450 km². In its lower reaches the
73 river averages 100 to 200 m wide and 2 to 3 m deep. Water discharge ranges from 5 m³ s⁻¹
74 during winter to 500 m³ s⁻¹ during the spring and early summer (Coachman, 1953).

75 This region of Labrador has experienced considerable RSL fall following retreat of the
76 Laurentide ice sheet over Goose Bay at ~8 ka (Syvitski and Lee, 1993). While, the initial RSL
77 fall rate was around ~50 mm yr⁻¹ (Clark and Fitzhugh, 1991), it has slowed to steady rate
78 between 3 and 10 mm yr⁻¹ over the last 5 ka (Fitzhugh, 1973; Clark and Fitzhugh, 1991). These

79 rates are also consistent with radiocarbon dating of stranded shorelines (Blake, 1955), and with
80 geodetic monitoring over the past two decades (Henton, et al., 2006).

81 **FIELD DATA COLLECTION and RESULTS**

82 We mapped four extant delta lobes within the Goose River system. At the mouth of the
83 Goose River there is an active, sandy delta (Fig. 1D), and upstream there are at least three
84 moribund delta lobes (Fig. 1A-C), as recognized by their lobate planform shape and visible
85 distributary channel networks. The median grain size is between 330 and 350 μm for all delta
86 lobes.

87 To constrain the timing of fluvio-deltaic deposition on the Goose River, we conducted a
88 topographic analysis using 30-m shuttle radar topography mission (SRTM) data and collected
89 sediment cores for OSL dating from delta lobes B and C (Fig. 1). We compared the accuracy of
90 the SRTM data with survey points from a fully corrected Leica 1320 global positioning system
91 and found good agreement with a root mean square error of less than 1 m. The sediment cores
92 for OSL dating (Fig. 1) came from overbank locations that were between distributary channels
93 (i.e. centers of mouth-bar areas) to minimize contamination from recent sediments deposited
94 during floods. Within the sediment cores, two samples were collected at different stratigraphic
95 elevations (Fig. DR1) to constrain lobe activity and aggradation rate. The single-aliquot
96 regenerative-dose (SAR) protocol (Murray and Wintle, 2000) was used to determine equivalent
97 doses (D_e) and subsequent OSL ages of each sample. Based on the character of the age
98 distributions, we used a central age model for the lobe B samples and the minimum age model
99 for lobe C samples (see data repository for more information on sample collection and OSL
100 dating).

101 Our OSL results and topographic analysis shows that during RSL fall the Goose River
102 avulsed to create at least three delta lobes at progressively lower elevations (Fig. 1 inset). OSL
103 ages suggest the Goose River delta avulsed from lobe B to C between 1 and 2 ka. During
104 deposition lobes B and C possessed vertical aggradation rates of ~ 4 and ~ 3 mm yr⁻¹, respectively.
105 Although we did not collect OSL samples for lobe A, we can estimate its age using the surface
106 elevation and the local sea-level curve. This method suggests it dates to ~ 3 ka.

107

108 **NUMERICAL MODELING SETUP AND RESULTS**

109 To understand the behavior of the Goose River in more detail we conducted a series of
110 modeling experiments of delta growth under RSL fall using Delft3D. Our model setup uses
111 boundary and initial condition measured on the Goose River. We simulate a fluvial system
112 entering a standing body of water with no tides, waves, or buoyancy forces. The river has a
113 constant bankfull discharge of $300 \text{ m}^3 \text{ s}^{-1}$ and carries an equilibrium concentration of $350 \mu\text{m}$
114 sediment. Along the seaward boundary we specify constant RSL fall rates varying from 0 to 10
115 mm yr⁻¹ (consistent with temporal variability at Goose Bay) using 1 mm yr⁻¹ increments and we
116 simulate rates of 16 and 20 mm yr⁻¹ to explore all of parameter space; this results in 13 runs total
117 (Table 1). Before RSL fall begins, a delta progrades basinward until the average topset slope
118 reaches dynamic equilibrium. We used this delta topography as the starting point for each RSL
119 fall scenario (see Data Repository for more information on model setup).

120 For analysis we mark the durations of all avulsions during RSL fall that create new,
121 distinct delta lobes. An avulsion is considered complete after water and sediment transported in
122 the initial delta lobe diminishes to zero. We define a delta lobe as a set of contemporaneous
123 channels feeding a topset of relatively constant elevation that is separated from neighboring

124 depocenters by an abrupt change in elevation (Fig. 2). We ignore the smaller intradelta lobe
125 avulsions (*sensu* Edmonds et al., 2009).

126 In our model runs, during RSL fall there is fluvio-deltaic deposition on the coastal plain
127 that is punctuated by fluvial avulsion (Figure 2A-C). This is consistent with observations on the
128 Goose River and recent work (Muto and Steel, 2004). No delta lobe avulsions occurred for runs
129 with RSL fall of 0 to 2 mm yr⁻¹. We find that avulsion period decreases with increasing RSL fall
130 rate (Fig. 2D). Avulsion number also increases with RSL fall, until a point is reached and they
131 decline rapidly (Figure 2D).

132 **DISCUSSION OF FIELD DATA AND MODELING**

133 Our field and numerical modeling results show that rivers can avulse and deposit multiple
134 delta lobes on the coastal plain during RSL fall. This result is significant as RSL fall should
135 suppress avulsions because channel incision, if fast enough, counteracts normalized
136 superelevation (height from water surface to sea-level relative to parent channel depth) that
137 commonly precedes avulsion (Slingerland and Smith, 2004).

138 We reason that avulsion can persist during RSL fall provided the channel becomes
139 superelevated. This would occur if the RSL fall signal does not cause enough incision in the
140 channel. This idea was quantified by Muto and co-workers (Muto and Steel, 2002, 2004; Muto
141 and Swenson, 2005, 2006; Swenson and Muto, 2007) who showed that a fluvio-deltaic system
142 will not incise when RSL falls if the fluvial response time τ is longer than the duration of RSL
143 fall T (i.e. $\tau > T$). Similarly, we define the fluvial response time as $\tau = \frac{q_s \cdot S}{r^2}$ where q_s is the
144 sediment supply per unit width of the active delta lobe (m² s⁻¹), S is the water surface slope, and r
145 is the rate of RSL fall (m s⁻¹). We take T to be the avulsion period, since that sets the duration a

146 given delta lobe is exposed to RSL fall, or in the case of no avulsions we use the total duration of
147 RSL fall.

148 Both the Goose River and our model runs with RSL fall of 1 to 10 mm yr⁻¹ possess τ/T
149 $\gg 1$ (Table 1) suggesting in these cases the fluvial system has not responded to RSL fall. This
150 is further supported by modeled channel bed elevations that show little incision (Fig. 3A). We
151 suggest avulsions continue because RSL fall superelevates the fluvial system, and also creates
152 surface gradient advantages where steeper delta front foresets are exposed due to shoreline
153 retreat. Consider that prior to the avulsion in Fig. 2C the channel does not incise (because τ/T
154 $\gg 1$, Table 1) and sea-level decreases faster than the water surface elevation in the channel.
155 This leads to a normalized superelevation of ~ 0.4 before avulsion (Fig. 3B), which is a
156 reasonable value for avulsion initiation in other systems (Hajek and Wolinsky, 2012). New delta
157 lobes are created as overbank flow accelerates down steeper pathways and forms incisional
158 avulsion channels (e.g., Hajek and Edmonds, 2014) (Fig. 3). Thus, the avulsion period decreases
159 with faster RSL fall rates because channels superelevate faster (Fig. 2D).

160 At higher RSL fall rates of 16 and 20 mm yr⁻¹ the model runs are characterized by $\tau/T < 1$
161 (Table 1). In these runs, the channel bed quickly erodes through the initial delta lobe (Fig. 4C),
162 entrenching the active channel and suppressing future avulsions. The few avulsions that do
163 occur arise from upstream migrating knickpoints that capture the river. The fluvial system
164 continues to deposit sediment and prograde as it follows the rapidly falling shoreline, but there
165 are no terraces and the surface grade is set by the RSL rate and underlying slope (Muto and
166 Swenson, 2006).

167 **IMPLICATIONS**

168 Our field and numerical results suggest that for a given fluvio-deltaic system, if $\tau/T \gg 1$
169 falling-stage deposits are characterized by a series of terraced, downstepping deltaic lobes,
170 whereas if $\tau/T \leq 1$ incision occurs through pre-existing lobes and falling-stage deposits lack well-
171 defined terraces ('smooth-topped' *sensu* Posamentier and Morris, 2000). These are some of the
172 first field-based results that verify the predictions of Muto and others (e.g. Muto and Steel, 2004)
173 and also illustrate that avulsion plays a key role in depositional mechanics during RSL fall.

174 Moreover, these results have important implications for sequence stratigraphic models.
175 Consider that sequence-bounding unconformities created during RSL fall may not always be an
176 erosive/bypass surface. Rather, deltaic lobe formation during RSL fall on the Goose River,
177 suggests that sediment is burying the unconformity as it forms ('cut and cover' model of
178 Holbrook and Bhattacharya, 2012). Though, it is admittedly not clear how much of this
179 deposition during RSL fall will be preserved in the geologic record. Our results also suggest
180 avulsion is an important process in emplacing falling-stage strata. Given this, the stratigraphic
181 architecture of falling-stage deposits depends on the rate of RSL fall, since the number of
182 terraced deltaic lobes scales with RSL fall rate (Fig. 2D). This result has implications for
183 reservoir properties, such as sand-body connectivity, which may decrease at higher rates of RSL
184 fall due to the presence of more terraced deltaic lobes.

185 **CONCLUSIONS**

186 The response of fluvio-deltaic systems to relative sea level (RSL) fall has received
187 considerable attention in the past, but new views, suggesting sediment deposition is common
188 (e.g. Muto and Steel, 2004, Swenson and Muto, 2007; Holbrook and Bhattacharya, 2012), are
189 emerging that require field and model verification. Herein, using observations of the Goose
190 River delta and Delft3D simulations, we have shown that fluvial avulsions can occur during RSL

191 fall. Optically-stimulated luminescence ages show that during RSL fall the Goose River delta
192 has avulsed on multiple times creating three delta lobes terraced at different elevations.
193 Numerical modeling with Delft3D shows that, similar to the Goose River delta, fluvio-deltaic
194 systems can produce avulsions and multiple terraced delta lobes during RSL fall. Avulsions
195 persist because the fluvial response time is slower than the duration of RSL fall, and rivers can
196 remain aggradational, causing superelevation and avulsions to occur during RSL fall. Moreover,
197 our modeling results suggest that the number and size of deltaic lobes scales with RSL fall,
198 suggesting that the sedimentary architecture of falling-stage deposits changes with the rate of
199 RSL fall.

200

201 ACKNOWLEDGEMENTS

202 The authors would like to thank A. Burpee, J. Royce, and A. McGuffin for field assistance. This
203 research was funded by NSF grants OCE-1061380 and EAR-1123847 awarded to DAE, OCE-
204 1061495 awarded to RLS, the Threet chair funds to JLB, and a Geological Society of America
205 student research grant to AGN. R. Somerville of the University of St Andrews is thanked for his
206 assistance with OSL samples.

207

208 ¹GSA Data Repository item 2014xxx, containing additional information on methods, is available
209 online at www.geosociety.org/pubs/ft2014.htm, or on request from editing@geosociety.org or
210 Documents Secretary, GSA, P.O. Box 9140, Boulder, CO 80301, USA.

211 REFERENCES CITED

212

213 Blake Jr, W., 1955, Note on the dating of terraces in the Lake Melville District, Labrador.
214 *Science*, v. 121 no. 3134, p 112.

215

216 Blake Jr, W., 1956, Landforms and topography of the Lake Melville area, Labrador,
 217 Newfoundland. Geography Bulletin, Department of Mines and Technical Survey,
 218 Ottawa, Canada, Volume 9, p 93-97.
 219

220 Catuneanu, O., 2006, Principles of sequence stratigraphy, Elsevier.
 221

222 Clark, P. U., & Fitzhugh, W. W., 1991, Postglacial relative sea level history of the Labrador
 223 coast and interpretation of the archaeological record, *in* Johnson, L.L., ed.,
 224 Paleoshorelines and prehistory: An investigation of method: Boca Raton, FL, CRC Press,
 225 189-213 p.
 226

227 Coachman, L. K., 1953, River flow and winter hydrographic structure of the Hamilton Inlet-Lake
 228 Melville Estuary of Labrador. Blue Dolphin Labrador Expedition – Winter Project 1953,
 229 19 p.
 230

231 Fitzhugh, W., 1973, Environmental Approaches to the Prehistory of the North: Washington,
 232 D.C., J. Wash. Acad. Sci, Volume 63, no. 2, 40 p.
 233

234 Hajek, E.A., and Edmonds, D.A., 2014, Is river avulsion style controlled by floodplain
 235 morphodynamics?: Geology, p. G35045. 35041.
 236

237 Hajek, E. A., and Wolinsky, M. A., 2012, Simplified process modeling of river avulsion and
 238 alluvial architecture: Connecting models and field data: Sedimentary Geology, v. 257, p.
 239 1-30.
 240

241 Helland-Hansen, W., and Hampson, G., 2009, Trajectory analysis: concepts and applications:
 242 Basin Research, v. 21, no. 5, p. 454-483.
 243

244 Henton, J. A., Craymer, M. R., Dragert, H., Mazzotti, S., Ferland, R., & Forbes, D. L., 2006,
 245 Crustal motion and deformation monitoring of the Canadian landmass. Geomatica, v. 60,
 246 no. 2, p 173-191.
 247

248 Holbrook, J. M. and J. P. Bhattacharya 2012, Reappraisal of the sequence boundary
 249 in time and space: Case and considerations for an SU (subaerial unconformity) that is not
 250 a sediment bypass surface, a time barrier, or an unconformity. Earth-Science Reviews
 251 **113**(3): 271-302.
 252

253 Li, Y. and J. P. Bhattacharya, 2013, Facies-Architecture Study of a Stepped, Forced
 254 Regressive Compound Incised Valley in the Ferron Notom Delta, Southern Central Utah,
 255 USA, Journal of Sedimentary Research, **83**(3): 206-225.
 256

257 Liverman, D.G.E. 1997, Quaternary Geology of the Goose Bay Area, Geological Survey Report
 258 97-1. Newfoundland Department of Mines and Energy, St. John's, pp. 173-182
 259

260 Murray, A. S., & Wintle, A. G., 2000, Luminescence dating of quartz using an improved single-
 261 aliquot regenerative-dose protocol. Radiation Measurements, v. 32, no. 1, p 57-73.

262
263 Muto, T., and Steel, R. J., 2002, In Defense of Shelf-Edge Delta Development during Falling and
264 Lowstand of Relative Sea Level: *The Journal of Geology*, v. 110, no. 4, p. 421-436.
265
266 Muto T., and Steel, R.J., 2004, Autogenic response of fluvial deltas to steady sea-level fall:
267 Implications from flume-tank experiments: *Geology*, v. 32, no. 5, p. 401-404.
268
269 Muto, T., and Swenson, J. B., 2005, Large-scale fluvial grade as a nonequilibrium state in linked
270 depositional systems: Theory and experiment: *Journal of Geophysical Research: Earth*
271 *Surface* (2003–2012), v. 110, no. F3.
272
273 Muto, T., and Swenson, J. B., 2006, Autogenic attainment of large-scale alluvial grade with
274 steady sea-level fall: An analog tank-flume experiment: *Geology*, v. 34, no. 3, p. 161-
275 164.
276
277 Posamentier, H. W., and Morris, W. R., 2000, Aspects of the stratal architecture of forced
278 regressive deposits: Geological Society, London, Special Publications, v. 172, no. 1, p.
279 19-46.
280
281 Romans, B. W., and Graham, S. A., 2013, A deep-time perspective of land-ocean linkages in the
282 sedimentary record: *Annual review of marine science*, v. 5, p. 69-94.
283
284 Slingerland, R. and N. D. Smith, 2004, River avulsions and their deposits, *Annual*
285 *Review of Earth and Planetary Sciences* **32**: 257-285.
286
287 Swenson, J. B., & Muto, T., 2007, Response of coastal plain rivers to falling relative sea-level:
288 allogenic controls on the aggradational phase. *Sedimentology*, v. 54, no. 1, p 207-221.
289
290 Syvitski, J. P., & Lee, H. J., 1997, Postglacial sequence stratigraphy of Lake Melville, Labrador.
291 *Marine Geology*, v. 143, no. 1, p 55-79.
292
293 Vail, P. R., 1977, Seismic stratigraphy and global changes of sea level, Part 4: Global cycles of
294 relative changes of sea level, *in* Seismic stratigraphy - applications to hydrocarbon
295 exploration. Mem. Amer. Assoc. Petrol. Geol., v. 26, p 83-97.
296
297 Van Heijst, M. W., & Postma, G., 2001, Fluvial response to sea-level changes: a quantitative
298 analogue, experimental approach. *Basin Research*, v. 13, no. 3, 269-292.
299

300

301 **Table 1:** Data used for τ/T calculations from Delft3D experiments and Goose River system. q_s

302 for Goose River is calculated from average sedimentation rates for lobes B and C derived from

303 OSL dated horizons. 3 mm yr^{-1} is considered to be a reasonable RSL fall rate for the Goose
304 River for the last 5 ka. Delft3D results consist of average conditions during the model run.

305
306 **Figure 1.** Google Earth image of the lower Goose River ($53^{\circ}21'48.32''\text{N}$, $60^{\circ}23'1.85''\text{W}$,
307 DigitalGlobe, June 14, 2012). Delta lobes A, B, C, and D are marked by black outline in the
308 large image. Delta lobes were defined by their distributary-channel networks and overbank
309 deposits. Inset plot shows spatially averaged elevation and ages of the four delta lobes (A-D).
310 Boxplots show SRTM elevation distributions, where solid horizontal lines and cross-hairs are the
311 median elevations and outliers for each lobe. The OSL age is listed below each boxplot. OSL
312 sample locations are marked on lobes B and C. Inset map shows the Goose River relative to Lake
313 Melville.

314
315 **Figure 2.** Serial maps of Delft3D simulation with a RSL fall of 3 mm yr^{-1} showing initial
316 condition (A) and two subsequent delta lobe avulsions (B, C). Elevations seaward of the delta
317 shoreline are clipped. Thick black lines indicate the position of the delta shoreline at the
318 previous time step. White boxes in A and B show the locations for measurements in Fig. 3A and
319 B, respectively. (D) Results of all Delft3D simulations show that as the rate of RSL fall increase,
320 avulsion period decreases, while number of avulsions (listed above each point) increase and then
321 decrease. Note that a RSL fall $\geq 3 \text{ mm yr}^{-1}$ is required to produce delta lobe avulsions.

322
323 **Figure 3.** (A) Spatially averaged channel bed elevations (η) at delta head remain roughly
324 constant for RSL fall rates below 10 mm yr^{-1} and become incisional at higher rates of RSL fall.
325 See Fig. 2A for location of spatial averaging. (B) In the time period prior to the lobe avulsion in
326 Fig. 2C, the normalized superelevation of the channel, defined as height from water surface to

327 RSL relative to channel depth, increases to ~ 0.4 before the avulsion occurs. The superelevation
328 occurs because RSL decreases faster than the water or bed surface. See Fig. 2B for location of
329 spatial averaging.

330

331

332

333

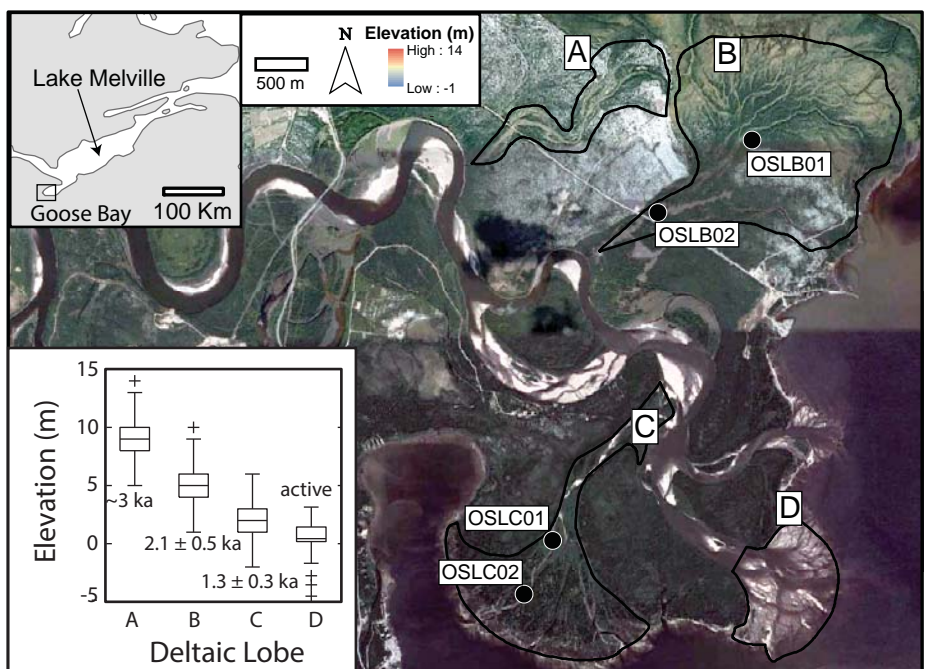


Figure 1. Google Earth image of the lower Goose River (53°21'48.32"N, 60°23'1.85"W, DigitalGlobe, June 14, 2012). Delta lobes A, B, C, and D are marked by black outline in the large image. Delta lobes were defined by their distributary-channel networks and overbank deposits. Inset plot shows spatially averaged elevation and ages of the four delta lobes (A-D). Boxplots show SRTM elevation distributions, where solid horizontal lines and cross-hairs are the median elevations and outliers for each lobe. The OSL age is listed below each boxplot. OSL sample locations are marked on lobes B and C. Inset map shows the Goose River relative to Lake Melville.

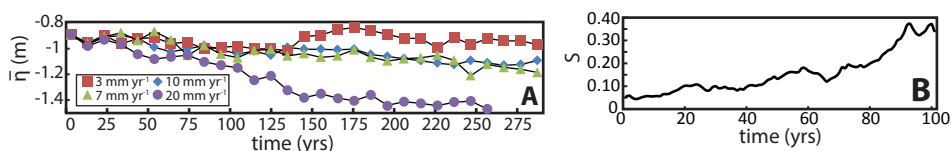


Figure 3. (A) Spatially averaged channel bed elevations (η) at delta head remain roughly constant for RSL fall rates below 10 mm yr⁻¹ and become incisional at higher rates of RSL fall. See Fig. 2A for location of spatial averaging. (B) In the time period prior to the lobe avulsion in Fig. 2C, the normalized superelevation of the channel (S), defined as height from water surface to RSL relative to channel depth, increases to ~ 0.4 before the avulsion occurs. The superelevation occurs because RSL decreases faster than the water or bed surface. See Fig. 2B for location of spatial averaging.

RSL fall (mm yr ⁻¹)	Number of avulsions	q_s (m ² s ⁻¹)	Slope	T (yrs)	τ (yrs)	τ/T
DELFT3D RUNS						
0	0	3.10E-06	2.11E-04	-	-	-
1	0	2.10E-06	2.16E-04	298.0	14260.3	47.9
2	0	2.06E-06	2.80E-04	298.0	4544.3	15.2
3	3	6.64E-06	3.06E-04	100.0	7130.7	71.3
4	4	1.03E-05	6.19E-04	74.8	12616.5	168.8
5	5	1.08E-05	9.07E-04	60.2	12363.6	205.4
6	6	1.61E-05	3.38E-04	49.7	4759.5	95.8
7	8	1.52E-05	7.89E-04	37.8	7707.6	204.2
8	7	1.74E-05	6.97E-04	43.0	5969.2	138.8
9	8	2.02E-05	1.20E-03	37.4	9461.7	253.2
10	9	2.75E-05	1.67E-03	33.4	14451.0	432.1
16	2	5.25E-06	1.40E-04	145.0	90.6	0.6
20	1	6.06E-06	1.70E-04	185.0	81.2	0.4
GOOSE RIVER (averages of lobes B and C)						
3.00	3	2.27E-07	2.30E-03	1000.0	1833.6	1.8

Table 1: Data used for τ/T calculations from Delft3D experiments and Goose River system. q_s for Goose River is calculated from average sedimentation rates for lobes B and C derived from OSL dated horizons. 3 mm yr⁻¹ is considered to be a reasonable RSL fall rate for the Goose River for the last 5 ka. Delft3D results consist of average conditions during the model run.

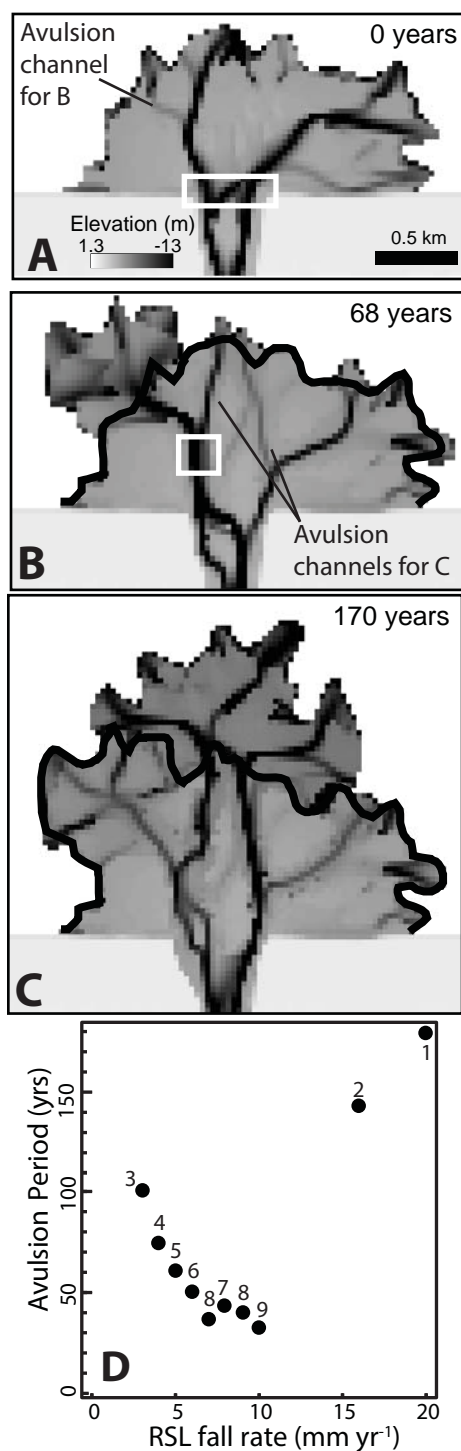


Figure 2. Serial maps of Delft3D simulation with a RSL fall of 3 mm yr⁻¹ showing initial condition (A) and two subsequent delta lobe avulsions (B, C). Elevations seaward of the delta shoreline are clipped. Thick black lines indicate the position of the delta shoreline at the previous time step. White boxes in A and B show the locations for measurements in Fig. 3A and B, respectively. (D) Results of all Delft3D simulations show that as the rate of RSL fall increase, avulsion period decreases, while number of avulsions (listed above each point) increase and then decrease. Note that a RSL fall ≥ 3 mm yr⁻¹ is required to produce delta lobe avulsions.